The biogeochemistry of tropical lakes: A case study from Lake Matano, Indonesia

Sean A. Crowe
Great Lakes Institute for Environmental Research, University of Windsor, Windsor, Ontario N9B 3P4, Canada; Earth and Planetary Sciences, McGill University, Montreal, Quebec H3A 2A7, Canada; GEOTOP-McGill-UQAM, Montreal, Quebec H3C 3P8, Canada

Andrew H. O'Neill
Great Lakes Institute for Environmental Research, University of Windsor, Windsor, Ontario N9B 3P4, Canada

Sergei Katsev[1]
Earth and Planetary Sciences, McGill University, Montreal, Quebec H3A 2A7, Canada; GEOTOP-McGill-UQAM, Montreal, Quebec H3C 3P8, Canada

Peter Hehanussa
Center for Limnology Research and Development, LIPI, Cibinong, West Java, Indonesia 16911

G. Douglas Haffner
Great Lakes Institute for Environmental Research, University of Windsor, Windsor, Ontario N9B 3P4, Canada

Bjørn Sundby
Earth and Planetary Sciences, McGill University, Montreal, Quebec H3A 2A7, Canada; ISMER, Université du Québec à Rimouski, Rimouski, Quebec G5L 3A1, Canada

Alfonso Mucci
Earth and Planetary Sciences, McGill University, Montreal, Quebec H3A 2A7, Canada; GEOTOP-McGill-UQAM, Montreal, Quebec H3C 3P8, Canada

David A. Fowle
Great Lakes Institute for Environmental Research, University of Windsor, Windsor, Ontario N9B 3P4, Canada; Department of Geology, University of Kansas, Lawrence, Kansas, 66047

Abstract

We examined the chemical composition of the water column of Lake Matano, Sulawesi Island, Indonesia, to document how the high abundances of Fe (hydr)oxides in tropical soils and minimal seasonal temperature variability affect biogeochemical cycling in lakes. Lake Matano exhibits weak thermal stratification, yet a persistent pycnocline separates an oxic epilimnion from anoxic meta- and hypolimnions. The concentration of soluble P in the epilimnetic waters is very low and can be attributed to scavenging by Fe (hydr)oxides. Chromium concentrations in the epilimnion are high (up to 180 nmol L^{-1}), but below U.S. Environmental Protection Agency guidelines for aquatic ecosystems. The concentration of chromium decreases sharply across the oxic–anoxic boundary, revealing that the hypolimnion is a sink for Cr. Flux calculations using a one-dimensional transport-reaction model for the water column fail to satisfy mass balance requirements and indicate that sediment transport and diagenesis play an important role in the exchange of Fe, Mn, P, and Cr between the epilimnion and hypolimnion. Exchange of water between the epilimnion and hypolimnion is slow and on a time scale similar to temperate meromictic lakes. This limits recycling of P and N to the epilimnion and removal of Cr to the hypolimnion, both of which likely restrict primary production in the epilimnion. Owing to the slow exchange, steep concentration gradients in Fe and Mn species develop in the metalimnion. These concentration gradients are

conducive to the proliferation of chemoautotrophic and anoxygenic phototrophic microbial communities, which may contribute a significant fraction to the total primary production in the lake.

Tropical lakes differ from their temperate counterparts in several important aspects. The higher annual irradiance, the lack of large seasonal variations in irradiance, and the smaller Coriolis effects at low latitudes combine to create weakly stratified lakes with relatively warm and uniform temperatures and low physical stability (Lewis 1987). The effects of latitude on the ecology of lakes are well documented (Lewis 1987; Reynolds et al. 2000), but the influence of latitude on the biogeochemistry of lakes has received much less attention. Nevertheless, two features can be expected to distinguish biogeochemical cycling in tropical lakes from that in temperate lakes: the absence of the temperature-driven convective overturn that annually oxygenates the entire water column in temperate lakes and significantly higher fluxes of allochthonous Fe and Mn (hydr)oxides resulting from intense chemical weathering in the catchments of tropical lakes.

Under low energy conditions, lakes are generally physically stratified: a surface layer (epilimnion) overlies a denser deep layer (hypolimnion) (Hutchinson 1957). Physically stratified lakes often exhibit chemical stratification. For example, when oxygen in the hypolimnion cannot be replenished as fast as it is consumed, microbial respiration switches to anaerobic pathways and redox stratification develops (i.e., the water column becomes stratified in terms of the distribution and speciation of redox-sensitive elements) (Hutchinson 1957; Wetzel 1983; Buffle and Stumm 1994). Anaerobic respiration typically proceeds first through NO_3^- reduction, followed by Mn(III/IV) and Fe(III) reduction, SO_4^{2-} reduction, and finally fermentation or methanogenesis (Stumm and Morgan 1996). The sequential use of oxidants (electron acceptors) generates gradients of electron acceptors, electron donors, and metabolites. These concentration gradients drive diffusive fluxes between layers and maintain chemical disequilibrium (Stumm and Morgan 1996). The oxidants Mn(III/IV) and Fe(III) typically exist as solid and colloidal (hydr)oxides with surfaces exhibiting both strong chemical affinities for many trace elements and large specific surface areas (Stumm and Morgan 1996). These Mn and Fe (hydr)oxides are susceptible to reductive dissolution (Stumm and Morgan 1996) and, therefore, the redox cycling of Fe and Mn can control the fate, distribution, and bioavailability of many trace elements (Buffle and Stumm 1994; Hamilton-Taylor and Davison 1995). Thus, Fe and Mn (hydr)oxides are not only important as terminal electron acceptors for anaerobic respiration but are also intimately linked to the biogeochemical cycling of many other minor and trace elements.

In this study we examine how the abundance of metal (hydr)oxides in catchment soils, the relative dearth of other electron acceptors, and the absence of marked seasonal temperature fluctuations influence biogeochemical cycling in tropical lakes as revealed by the chemistry of the water column in Lake Matano, Indonesia.

Regional setting

Lake Matano is part of the Malili Lakes system of Indonesia. The Malili Lakes are situated on Sulawesi Island and constitute a morphologically diverse group that includes Lake Matano, Lake Mahalona, Lake Towuti, Lake Lawontoa, and Lake Masapi. To date, Lake Matano is the most extensively characterized (Lehmusluoto et al. 1999; Haffner et al. 2001; Crowe et al. 2004). Lake Matano is tectonic in origin and is hosted by a cryptodepression with a graben structure. More than 590-m deep, Lake Matano is among the 10 deepest lakes in the world. The lake is 28-km long, 8-km wide, and has a relatively small surface area (164 km²). It has been suggested, based on geological and biological information, that Lake Matano is between one and four million years old (Brooks 1950). Owing to the relatively steep regional topography (the highest point in the catchment is 1,400–1,700 m above sea level [a.s.l.], the lake surface is at 382 m a.s.l.), the total catchment area of Lake Matano is relatively small (~436 km²). The surficial geology of the catchment basin is dominated by nickeliferrous lateritic soils (which contain up to 60% iron oxides) that have developed on ultramafic rocks of ophiolitic origin (Golightly 1981). As a result, the sediments of the Malili Lakes are Fe-rich and can contain more than 20 weight percent Fe (hydr)oxides (Crowe et al. 2004). In addition to the ultramafic rocks, limestones and cherts outcrop along the southern shore of Lake Matano. The regional climate is humid–tropical and lacks marked seasonal temperature fluctuations or year-to-year variability (Hope 2001). The region around Lake Matano receives an average rainfall of 2,737 mm per year and has an average temperature of 24°C with a range of 22–31°C (Hope 2001). The Malili Lakes are the principal freshwater resource in the region and also host a unique and diverse aquatic ecosystem (Von Rintelen and Glaubrecht 2003; Roy et al. 2004; Herder et al. 2006). Ancient lakes, such as Lake Matano, have relatively stable physical characteristics and are therefore conducive to the development of high degrees of species endemism. The Malili Lakes have been cited as ''a superb natural laboratory'' for studying evolutionary processes and have been likened to the aquatic equivalent of the Galapagos Islands (F. Herder pers. comm.). In addition, Myers et al. (2000) have identified Sulawesi as a ''hotspot'' for biological conservation based on the two criteria of exceptionally high concentrations of endemic species and rapid habitat loss. Though Lake Matano is characterized by very high degrees of endemism, the species richness and endemicity are not matched by high levels of productivity (Sabo 2006). The standing crops of phytoplankton in Lake Matano are very low (0.013 mg L^{-1}), even compared with ultraoligotrophic lakes such as Great Bear Lake (0.06–0.09 mg L^{-1}) in the Canadian Arctic (Sabo 2006). It has been proposed that the low levels of primary production in Lake Matano, and the Malili

Lakes in general, result from a combination of both nutrient limitation and metal toxicity (Sabo 2006).

Iron and manganese are abundant in the soils of the Malili Lakes catchment area, and thus Fe and Mn redox cycling may be especially important in regulating the chemical composition of Lake Matano (Crowe et al. 2004). Previous studies reported that the deep waters of Lake Matano are characterized by low oxygen concentrations (Lehmusluoto et al. 1999; Haffner et al. 2001), but the presence of a suboxic to anoxic hypolimnion remained speculative. The absence of strong seasonal temperature fluctuations on Sulawesi Island precludes seasonal convective overturn as a mechanism to transport oxygen into the deep waters of Lake Matano. The main seasonality on Sulawesi Island, and in the tropics in general, is in the amount of precipitation delivered during the wet (October–June) and dry (July–September) seasons. Intense precipitation during the wet season coupled with the steep topography around Lake Matano suggests that runoff may contribute to mixing (Haffner et al. 2001) and may generate lateral intrusions of oxygen-rich water into deeper waters in a situation partly analogous to the Bosporus plume in the Black Sea (Konovalov et al. 2003). Given the great depth of Lake Matano, its mountainous setting, and its moderate surface area (short fetch), it is unlikely that local winds could generate sufficient energy to mix the water in the deep basins of Lake Matano.

Methods

Sampling and storage—Sampling was conducted at a central deep-water location ($2°28'00''$S and $121°17'00''$E, Fig. 1) in August–September 2004 (end of the dry season) and June–July 2005 (end of the wet season) aboard the R/V *Watu Lonto*. Water samples were collected using 5-liter Go-Flow (Niskin) bottles attached in series to a stainless steel airline cable and a hand winch. Bottles were placed at depth to an accuracy of ± 5 m using a commercial sonar device to monitor the position of the bottles within the water column. Once at the surface, the Niskin bottles were subsampled according to U.S. Environmental Protection Agency guidelines (USEPA 1983). Unfiltered water samples were transferred directly to a voltammetric cell for electrochemical analyses or to acid-washed high-density polyethylene (HDPE) bottles (14% v/v HNO_3 for 24 h followed by quadruplicate rinsing in Milli-Q [MQ] water and drying in class 1000 laminar flow hood) via acid-washed Tygon tubing. Other water samples were filtered after drawing the water into an acid-washed 60-mL syringe through the Tygon tubing. Waters were filtered through 0.45-μm (Whatman) and/or 0.02-μm (Millipore) polypropylene syringe filters directly into HDPE bottles. There was no significant difference between concentrations (Fe(II), Mn, Cr, Ni, Co, P) in the 0.02- or 0.45-μm filtrates. In the rest of the text the term "dissolved" refers to material passing through a 0.02-μm filter. All samples were transported to the field station and acidified to 1% equivalent volume with trace-metal grade HNO_3 (purified by subboiling distillation) within 8 h of sampling. Unfiltered samples were not digested, but acidification to 1%
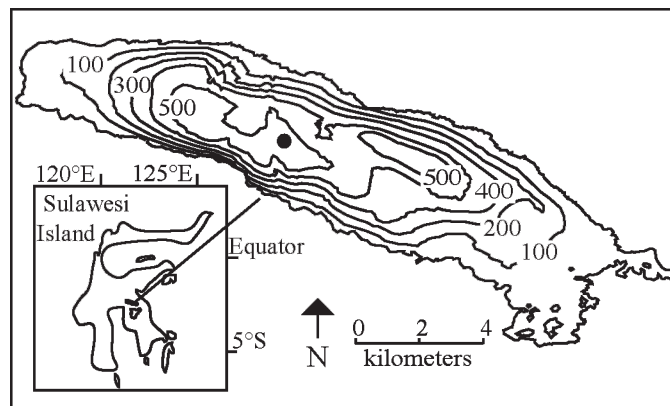

Fig. 1. Lake Matano bathymetry. The circle marks the position of the deep-water master sampling station. Modified from Haffner et al. (2001).

(pH <2) with HNO_3 should dissolve most of the inorganic particulate material with the exception of crystalline silicates and some clay minerals. Concentrations determined by analyses of acidified, unfiltered samples are hereafter referred to as "total" concentrations despite the fact that some refractory material may not have been digested. All samples were refrigerated and maintained at $4°C$ until analysis.

Methods of analysis—Water temperature, conductivity, and pH profiles were collected in situ using a submersible conductivity–temperature–depth sensor (RBR). Measurements of dissolved oxygen were also conducted in situ to a depth of 100 m using a Clark-type electrode, calibrated to 100% saturation in air, fixed to a multiparameter probe (Hydrolab). Oxygen measurements at deeper depths were made by linear sweep voltammetry (*see below*) on whole water samples collected using the Niskin bottles. Eh (2004 only) was measured on whole water samples with a VWR SympHony SP301 meter using an Orion 96–78 combination electrode (Ag-AgCl reference) calibrated with Zobell's solution and corrected to the standard hydrogen electrode (SHE). The colorimetric methods described below were conducted on site using a Hach DR2010 spectrophotometer. Fe(II) was determined using a modified version of the ferrozine method (Viollier et al. 2000). Alkalinity (2005 only) was determined using the colorimetric method described by Sarazin et al. (1999). In 2004, nitrogen species (i.e., NO_3^-, NO_2^-, and NH_4^+) were determined using Hach Accuvac ampuls (Nitra/Nitriver 5LR) and the Hach ammonium–nitrogen salicylate kit. In 2005, nitrogen species were determined by ion chromatography (Dionex), on samples preserved by acidification (to 1% equivalent volume H_2SO_4), using an IonPAC ASHC-11 column with conductivity detection (Dionex CD-25).

An Analytical Instrument Systems (AIS) DLK-60 with cell stand was used for all electrochemical analyses. Voltammetric measurements were conducted with a three-electrode configuration using a Au-Hg amalgam microelectrode (50-μm radius), a saturated Ag-AgCl, and a platinum wire as the working, reference, and counter electrodes, respectively (Brendel and Luther 1995). The

voltammetric techniques used in this work are described by Luther et al. (2003). Briefly, dissolved O_2 was measured by linear sweep (LS) voltammetry, and Fe(II), Mn(II), S(-II) species, and organo-Fe(III) were measured by square-wave voltammetry. The detection limits are 5, 15, 5, and <0.2 μmol L^{-1} for O_2, Fe(II), Mn(II), and HS^- respectively (Luther et al. 1998). As discussed by Taillefert et al. (2000), it is not possible to calibrate quantitatively for organo-Fe(III). The macroelements (Ca, Mg, Si, and Mn, Fe, and P in the bottom waters) were determined by inductively coupled plasma–optical emission spectrometry (ICP-OES; Thermo Jarrell Ash). Trace metals and P were determined by inductively coupled plasma–mass spectrometry (ICP-MS) using either a ThermoElemental X7 (2004 samples) or an Elan 6100 plus (2005 samples). Mass bias corrections were made using a three element internal standard (Be, In, Tl, or Bi). Instrumental detection limits were calculated as three times the standard deviation of eight measurements of MQ water containing the internal standards in an acid matrix (P = 0.05, Fe = 0.02, Mn = 0.003, Cr = 0.03, Co = 0.00015, Ni = 0.008 all in μmol L^{-1}). Estimates of the precision and accuracy of the measurements were made by repeated analyses of the riverine water standard reference material (SLRS-4) and both epilimnetic and hypolimnetic waters (precision, P < 5%, Fe < 1%, Mn < 3%, Cr < 1%, Co < 2%, Ni < 1% relative standard deviation (RSD); accuracy, better than 5% all elements).

Speciation calculations and stability diagrams were obtained using the JChess geochemical modeling software (Van Der Lee 1993) and the MINTEQA2 thermodynamic database (Allison et al. 1991).

Results and discussion

In this section, we describe the physical characteristics of the lake that pertain to mixing and oxygen transport in the water column; evaluate trace element redox speciation in the lake water using measured pE and pH profiles in combination with thermodynamic equilibrium calculations; and use reaction-transport modeling to provide a quantitative description of the rates of biogeochemical cycling. Emphasis is placed on the fate and distribution of macronutrients and heavy metals so that future studies can more readily identify the factors that regulate the biological composition and productivity of this and other tropical lakes as well as their capacity to buffer increasing anthropogenic stresses. A representative compilation of the data presented in the figures is available in tabular format online (*see* Web Appendix 1: www.aslo.org/lo/toc/vol_53/issue_1/0319a1.pdf).

Physical characteristics—Lake Matano water density was calculated from profiles of temperature and conductivity (Imboden and Wüest 1995) collected at the end of the 2004 dry season and the end of the 2005 wet season. Stratification in both temperature and total dissolved solids resulted in a well-developed pycnocline at ~100-m depth and a metalimnion that extended from 100-m to ~220-m depth during both seasons (Fig. 2). Most of the density gradient was generated by the temperature gradient, but the
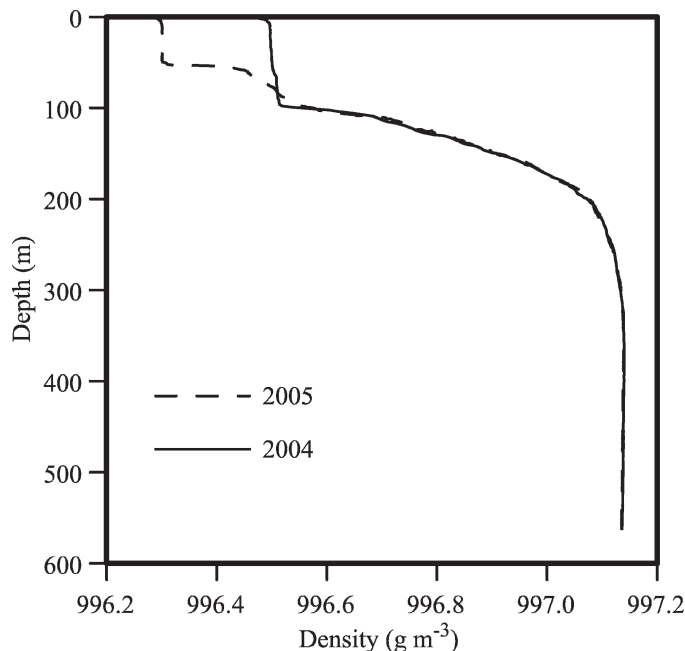

Fig. 2.   Density as a function of depth at the end of the dry season 2004 and the end of the wet season 2005.

difference between the total dissolved solids concentration (TDS, estimated from conductivity; Langmuir 1997) in the epilimnion and hypolimnion accounted for approximately 20%. Although the thermal stratification was relatively weak compared with seasonally stratified temperate lakes, the TDS gradient imparted additional stability to the stratification: the epilimnetic waters would need to cool to less than 25°C (0.5°C degrees below the hypolimnion temperature) to achieve homogenous density throughout the water column. The similarity of the density profiles between the wet and dry seasons and between 2004 and 2005, as well as the accumulation of TDS in the hypolimnion, suggests that the lake has not been vertically mixed recently. Nevertheless, it is difficult to estimate how long it has been since complete vertical mixing occurred.

The higher concentration of dissolved solids in the hypolimnion was due to higher concentrations of HCO_3^-, which were largely balanced by equivalent increases in Ca^{2+}, Mg^{2+}, and Fe^{2+} concentrations. The higher concentration of HCO_3^- most likely originated from the accumulation of heterotrophic respiration products, but higher concentrations of dissolved Mg^{2+} and Ca^{2+} probably arose from their release during the reductive dissolution of Fe (hydr)oxide carrying phases (Sholkovitz 1985). These observations are consistent with biogenic meromixis, a feature common to deep equatorial lakes (Wetzel 1983).

Redox stratification—Vertical profiles of oxygen (Fig. 3a) show that in both 2004 and 2005, oxygen was only measurable to a depth of 100 m. Oxygen was below the detection limit of linear sweep voltammetry (5 μmol L^{-1}) in deeper samples (110, 120, 140, 160, 180, 500 m). The discrepancy in the oxygen concentration profiles in the epilimnion between the two samplings was due to

differences in the mixing regime and is consistent with the presence of a seasonal pycnocline that developed during the wet season. This seasonal pycnocline developed due either to a decrease in evaporative cooling or lower wind stress during the rainy season.

Below 100 m, the concentrations of dissolved Mn increased sharply to a maximum of 9.5 μmol L^{-1} at 110 m, whereas dissolved Fe(II) concentrations increased to a maximum of 140 μmol L^{-1} at 300-m depth (Fig. 3b). The latter are at the upper end of the range of concentrations reported for suboxic freshwaters (Hamilton-Taylor and Davison 1995). The virtually identical profiles of dissolved Fe and Mn over consecutive years of sampling imply that redox stratification persists over annual and likely longer time scales. This is consistent with the well-developed density stratification and slow mixing through the metalimnion. The invariance of the Fe and Mn profiles further suggests that steady-state redox conditions prevailed.

The concentrations of dissolved Mn and Fe were approximately constant at 6.4 and 140 μmol L^{-1} respectively, below 300-m depth. Saturation indices (SI) with respect to common mineral phases for water at 300-m depth are presented in Table 1. The index is given by

$$SI = \log \left[\frac{IAP}{K_{sp}} \right] \qquad (1)$$

where IAP is the ion activity product and K_{sp} is the solubility product of a given mineral phase at the same temperature and pressure. According to these calculations, Lake Matano bottom waters were supersaturated with respect to magnetite, hematite, maghemite, ferrihydrite, strengite, and siderite. The precipitation of these minerals should buffer the aqueous concentrations of Fe, Mn, PO_4^{3-}, and CO_3^{2-}, therefore regulating the influence of increased or decreased input fluxes.

The dominant N, Mn, Fe, and S species can be predicted using thermodynamic equilibrium calculations that can be visualized in pE-pH predominance diagrams (Stumm and Morgan 1996). Plots of pE, calculated from field measurements of Eh, versus pH (Stumm and Morgan 1996), along with stability fields for Lake Matano waters, are shown in Fig. 4. These diagrams reveal that Lake Matano waters exhibit a bimodal distribution in terms of pE and pH with lower values in the hypolimnetic waters. The equilibrium calculations predict that NO_3^- should be the dominant dissolved (nongaseous) species in the epilimnion and that NH_4^+ should dominate in the hypolimnion. Very low concentrations of N precluded the quantitative determination of N species in the epilimnetic waters, but >10 μmol L^{-1} NH_4^+ was detected in the hypolimnion (data not shown). With respect to Mn, the epilimnetic waters plot in the stability field of poorly soluble Mn (hydr)oxide (MnO_2), whereas under the reducing conditions encountered in the hypolimnion, Mn(III/IV) (hydr)oxides should reductively dissolve to Mn(II). Indeed, the concentration of dissolved Mn increased sharply below the redoxcline (Fig. 3). With respect to Fe, the epilimnetic waters plot largely in the stability field of poorly soluble (hydr)oxides
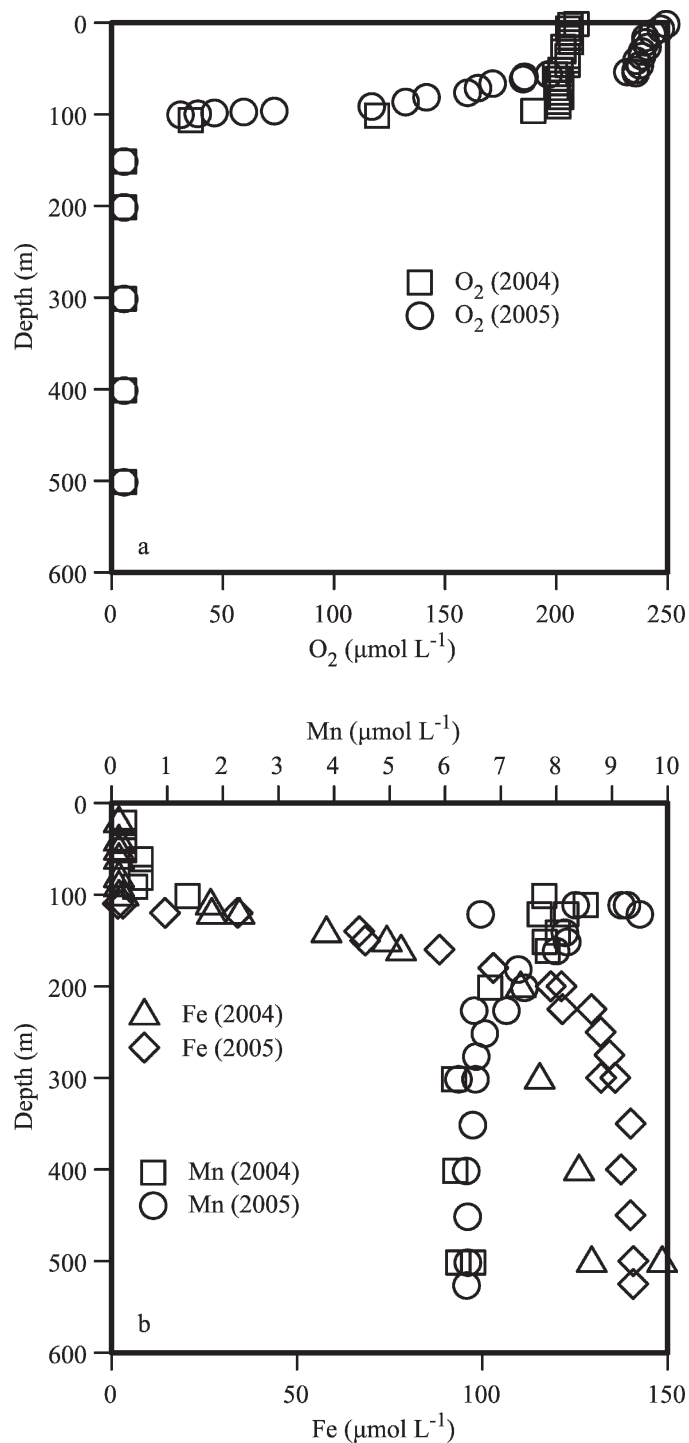

Fig. 3. (a) Vertical profiles of dissolved oxygen from 2004 and 2005. (b) Vertical profiles of dissolved (<0.45 μm) Fe and Mn from 2004 and 2005. Note that measurements of dissolved Fe(II) are indistinguishable from dissolved total Fe.

$(Fe(OH)_3)$, as is also the case for Mn. The hypolimnetic waters plot near the boundary between the oxidized species $Fe(OH)^{2+}$ and the reduced aqueous species Fe^{2+}. Accordingly, the redox potential of the hypolimnetic waters appears to be buffered by the Fe^{2+}-$Fe(OH)^{2+}$ redox couple. High concentrations of dissolved Fe(II) were observed in

Table 1.   Saturation indices calculated for 300 m depth (2005).

Mineral	Chemical formula	SI
Magnetite	Fe_3O_4	22.13
Hematite	Fe_2O_3	20.63
Maghemite	Fe_2O_3	10.19
Goethite	$FeOOH$	9.311
—	$Fe_3(OH)_8$	5.572
Ferrihydrite	$Fe(OH)_3$	3.399
Strengite	$Fe(PO_4)_2 \cdot H_2O$	2.722
—	$MnHPO_4$	1.885
Siderite	$FeCO_3$	0.3443
Rhodocrosite	$MnCO_3$	−0.068
Vivianite	$Fe_3(PO_4)_2$	−0.2992
Calcite	$CaCO_3$	−0.747
Aragonite	$CaCO_3$	−0.89
Dolomite	$CaMg(CO_3)_2$	−1.012
Hydroxyapatite	$Ca_{10}(PO_4)_6(OH)_2$	−2.752

(Fig. 5). This sulfide may originate from the degradation of S-bearing organic matter, or emanate from the underlying sediment, but sulfate reduction would only occur in sediments overlain by water containing sulfate. Therefore, only sediments within a narrow depth interval below the pycnocline could be a source of sulfide to the water column. The peak shape of the sulfide profile (Fig. 5) in the vicinity of the pycnocline can be explained by sulfide oxidation at depths less than 120 m and the precipitation of FeS resulting from the reaction of HS^- with upward diffusing Fe(II) at depths below 120 m. The presence of sulfide in the hypolimnion may be important in governing Ni and Co cycling (*see below*).

Origin and distribution of organic matter in the water column—Redox stratification is linked to the microbially mediated oxidation of organic matter. Owing to the low primary productivity in Lake Matano (Lehmusluoto et al. 1999; Haffner et al. 2001; Sabo 2006), the organic matter content of the water column is very low. The autochthonous particulate organic carbon (POC) component, estimated from the biomass given in Sabo (2006) (assuming Redfield organic matter stoichiometry: $C:N:P = 106:16:1$; Redfield et al. 1963), is less than 1 μmol L^{-1}

the hypolimnion (Fig. 3). Both epilimnetic and hypolimnetic waters plot within the stability field of SO_4^{2-} (Fig. 4), suggesting that sulfate reduction should not occur in the water column. Nevertheless, trace concentrations of free sulfide were detected immediately below the redoxcline
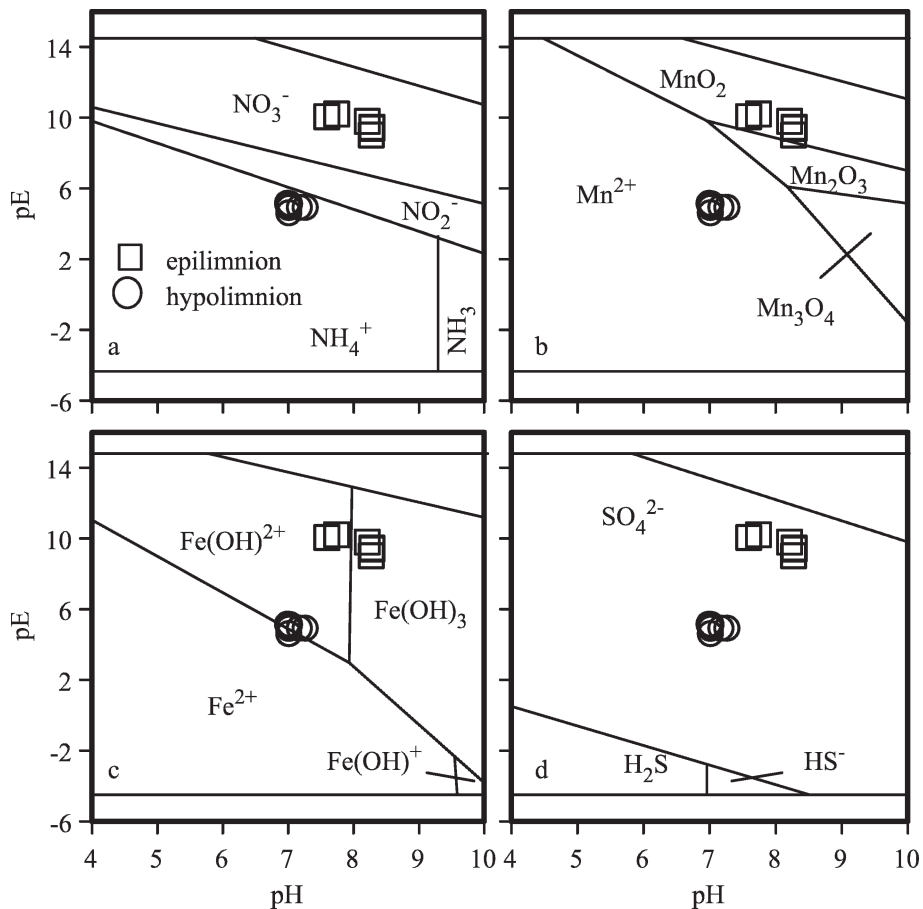

Fig. 4.   pE versus pH diagrams for species of (a) nitrogen, (b) manganese, (c) iron, and (d) sulfur. Symbols are pE–pH coordinates for selected samples of Lake Matano waters. The bimodal distribution represents waters from the hypolimnion with low pE and pH values and waters from the epilimnion at relatively higher values.
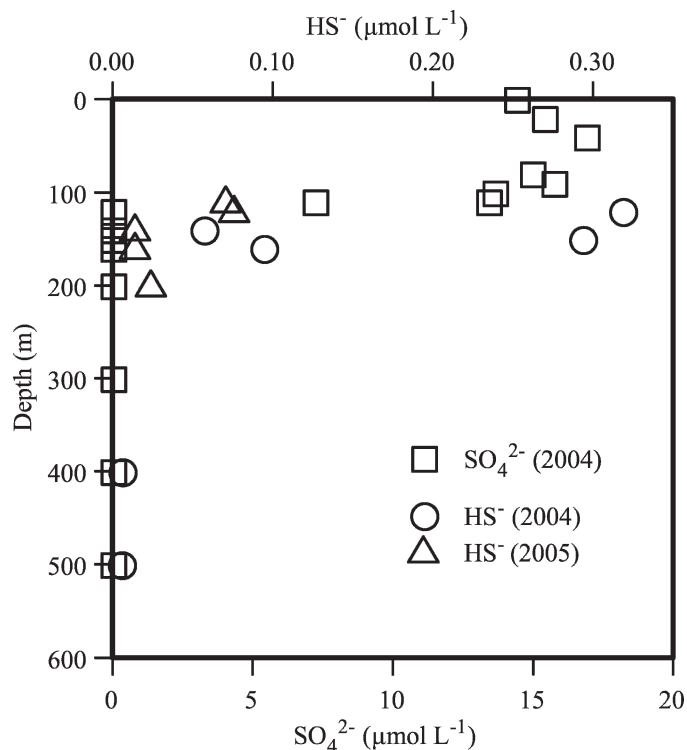
Fig. 5. Profiles of dissolved HS^- (2004 and 2005) and dissolved sulfate (2004 only).

and is mostly remineralized within the epilimnion (Haffner et al. 2001). This implies that redox cycling in Lake Matano is likely driven by allochthonous organic matter. Dissolved organic carbon (DOC) concentrations (Haffner unpubl. data) in the epilimnion are uniform and approximately 1,000 μmol L^{-1} but decrease to <100 μmol L^{-1} below 100-m depth. The sharp concentration gradient across the metalimnion should drive a strong flux of DOC to the hypolimnion. Taken together these observations suggest that redox cycling in Lake Matano is fueled by allochthonous DOC and that DOC is almost completely mineralized by anaerobic respiration within a narrow depth interval between 100 and 200 m. The depth interval in which dissolved Fe(II) increased coincides with the depth interval of DOC mineralization and suggests that DOC is mineralized predominantly via Fe reduction. This situation may be unique to tropical lakes that have catchments rich in Fe (hydr)oxides and that are poor in more energetic electron acceptors.

Phosphorus and trace-metal distribution and speciation— The concentrations of both soluble reactive phosphate (SRP) and total P were below our detection limit (0.05 μmol L^{-1}) in the epilimnion, but SRP increased concomitantly with dissolved Fe(II) in the metalimnion (Fig. 6). The ratio of dissolved Fe to dissolved P was approximately 16:1 in the metalimnion and remained relatively constant with depth. This suggests that the geochemistry of P in Lake Matano is intimately linked to the Fe cycle and that the P concentration in the epilimnion is likely limited by sorption to particulate or colloidal Fe
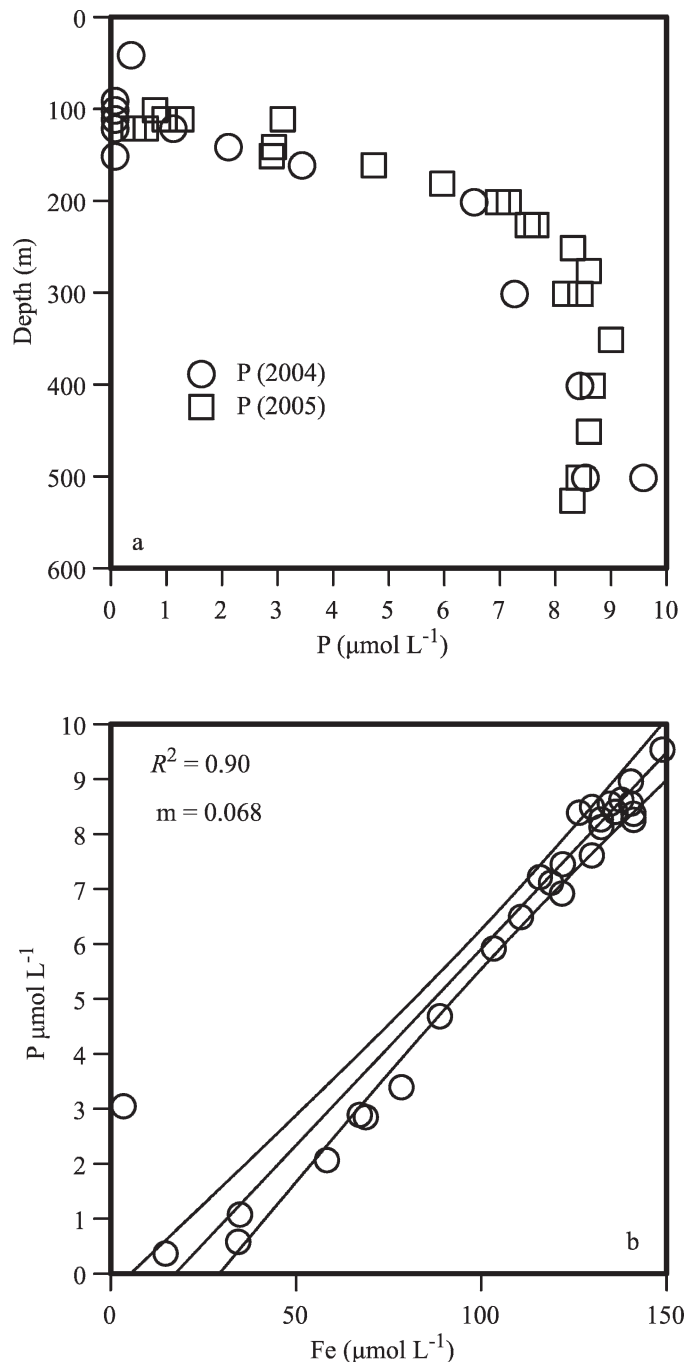

Fig. 6. (a) Profile of soluble reactive phosphate (SRP) from 2004 and 2005. (b) SRP as a function of dissolved (<0.45 μm) Fe for 2004 and 2005 (not distinguished). The confidence band on the linear regression represents the 95% interval.

(hydr)oxides. Assuming a 30-Å particle size, Anschutz et al. (1998) estimated that ferrihydrite (a poorly crystalline Fe (hydr)oxide) could sorb phosphate up to a molar Fe:P ratio of 6.7. Therefore, the ratio of dissolved Fe:P in the hypolimnion of Lake Matano (16:1) suggests that either (1) the Fe (hydr)oxides supplying ferrous Fe and P to the meta- and hypolimnions were undersaturated in P, (2) the Fe (hydr)oxides were dissolving incongruently with P being

preferentially incorporated into a secondary mineral or retained in a refractory Fe (hydr)oxide component, or (3) P was taken up in biomass. The low POC concentrations negate biological uptake and imply either undersaturation of Fe oxyhydroxide surfaces in P or secondary precipitation of minerals with low Fe : P ratios like strengite (Fe : P = 1 : 1) or $MnHPO_4$ (Fe : P = 0 : 1). Both strengite and $MnHPO_4$ are supersaturated in the hypolimnion (Table 1).

The concentration of dissolved Cr in the epilimnion was uniform at ~180 nmol L^{-1} and virtually identical in both 2004 and 2005 (Fig. 7a). Speciation calculations reveal that at equilibrium most of this Cr should be in the hexavalent state (Fig. 7b). The Cr(VI) concentration was below USEPA guidelines (criterion continuous concentration [CCC]; USEPA 2006). The CCC is an estimate of the highest concentration of a substance in surface water to which an aquatic community can be exposed indefinitely without resulting in an unacceptable effect (USEPA 2006). It is thus unlikely that the presence of Cr(VI) is solely responsible for the low productivity in Lake Matano. Dissolved Cr concentrations decreased dramatically below 100-m depth to less than our detection limit of 30 nmol L^{-1}. The decrease is consistent with the reduction of Cr(VI) to the less soluble and more particle reactive Cr(III) by Fe(II) (Johnson et al. 1992). Thermodynamic equilibrium calculations predict that, in the presence of micromolar concentrations of Fe, chromite ($FeCr_2O_4$) should precipitate from the hypolimnetic waters. However, laboratory experiments with Fe-reducing bacteria have shown that the dominant product of Cr reduction by ferrous Fe is a mixed Fe, Cr (hydr)oxide ($Fe_{1-x}Cr_x(OH)_3 \cdot nH_2O$) (Hansel et al. 2003). Hansel et al. proposed the following reaction to describe the precipitation of Cr induced by the reaction with Fe(II):

$$3Fe^{2+} + CrO_4^{2-} + 8H_2O \Leftrightarrow 4Cr_{0.25}Fe_{0.75}(OH)_3 + 4H^+$$

Such an amorphous Cr-Fe (hydr)oxide may be more reactive toward reoxidation to Cr(VI) than chromite if mixed into the zone of Mn oxidation.

The concentration of dissolved Ni was relatively high (~60 nmol L^{-1}) throughout the water column, but it peaked at 210 nmol L^{-1} near the pycnocline, likely as a result of the reductive dissolution of particulate Mn (hydr)oxides (Figs. 3b, 8). Mn (hydr)oxides have a strong affinity for Ni (Manceau et al. 1992, 2003, 2005) and serve as carrier phases for this and many other elements (e.g., Mo). Similar to Mn and Fe, dissolved Co concentrations were also very low in the epilimnion. They increased concomitantly with Fe ($R^2 = 0.77$) in the metalimnion (Figs. 3b, 8). The much greater abundance of Ni than Co in the catchment area soils (Golightly 1981) may explain why the concentration of Ni was higher than Co in the epilimnion. In contrast to the concentration of Co, which increased in concentration below the redoxcline, the concentration of Ni decreased by ~30%. The concentrations of Ni and Co were almost identical below 150-m depth and remained constant at ~40 nmol L^{-1} below 200 m. This similarity within the anoxic hypolimnion suggests that dissolved Ni and Co concentrations are
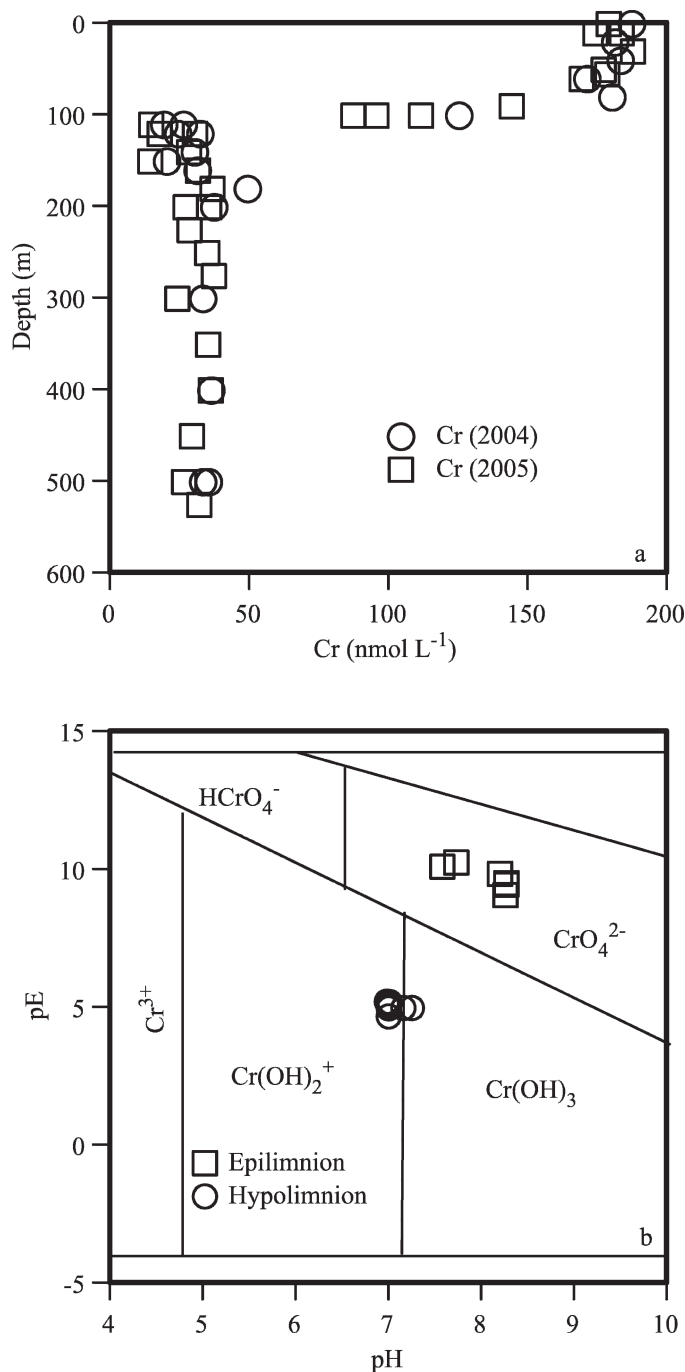

Fig. 7. (a) Vertical profiles of dissolved (<0.45 μm) Cr from 2004 and 2005. (b) pE vs. pH diagram for Cr species. The bimodal distribution represents waters from the hypolimnion with low pE and pH values and waters from the epilimnion at relatively higher values.

buffered by incorporation into a solid phase. Solid phases with the potential to incorporate Ni and Co include Fe, Mn, and Ca carbonate or phosphate minerals; authigenic oxides of Fe; and sulfide minerals. Despite the apparently minor role for sulfate reduction in organic matter oxidation within the water column, small amounts of sulfate reduction could play an important role in the dynamics of
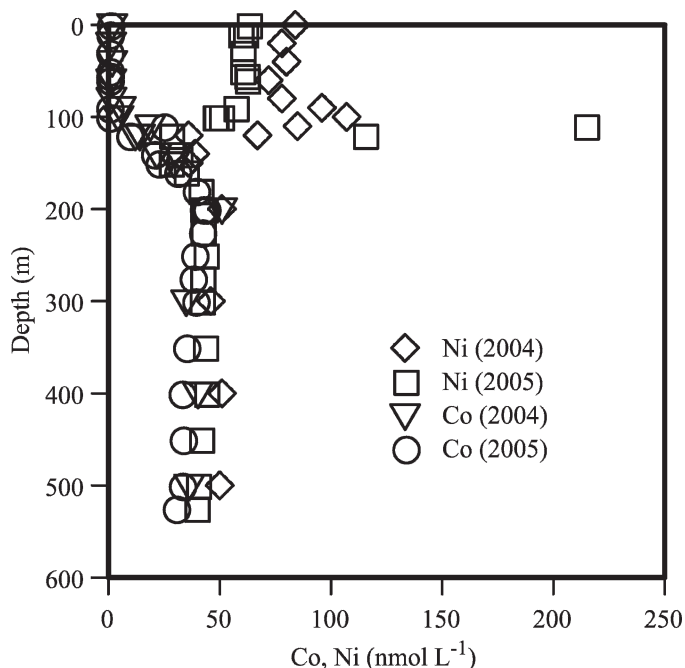
Fig. 8. Vertical profiles of dissolved (<0.45 μm) Ni and Co from 2004 and 2005.

Fig. 9. Saturation indices for Ni and Co monosulfides as a function of HS$^-$ concentration. The solid line at SI = 0 corresponds to equilibrium, above the line Ni and Co monosulfides are expected to precipitate and below the line dissolve. The shaded area delineates the sulfide concentrations present in Lake Matano.

trace metals. Speciation and saturation index calculations over a range of sulfide concentrations, pH = 7.00, HCO$_3^-$ = 2 mmol L^{-1} (Fig. 9), reveal that at dissolved Ni concentrations of 50 nmol L^{-1}, waters become saturated with respect to Ni monosulfide (NiS, milerite) at sulfide concentrations as low as 50 nmol L^{-1}. In contrast, at dissolved Co concentrations of 50 nmol L^{-1}, water remains undersaturated with respect to Co monosulfide until the sulfide concentration is nearly one order of magnitude greater (Fig. 9). This reflects the lower solubility of NiS (K_{sp} = 10$^{-8.0345}$) than CoS (K_{sp} = 10$^{-7.374}$). Concentrations of dissolved sulfide in the hypolimnion of Lake Matano were within the range necessary to induce NiS precipitation but not to precipitate CoS. Although the high concentrations of Fe(II) in the hypolimnion would effectively scavenge any free sulfide, the solubility of FeS is much higher than either NiS or CoS. Therefore, the presence of dissolved Fe(II) would not inhibit NiS or CoS precipitation until the concentration of Fe(II) is over 1 mmol L^{-1}.

One-dimensional description of Fe cycling—The uniform increase in dissolved Fe(II) concentrations within the metalimnion suggests the presence of a source and a sink for Fe(II) within this depth interval. To quantify the rates of Fe cycling in the metalimnion we analyzed the available concentration data with a one-dimensional reaction-transport model that includes (1) sinking of particulate Fe(III) (hydr)oxides through the metalimnion; (2) reductive dissolution of Fe(III) (hydr)oxides coupled to organic matter oxidation in the metalimnion; (3) upward diffusion of Fe(II) toward the epilimnion; and (4) Fe(II) oxidation and the reprecipitation of Fe(III) (hydr)oxides at the upper boundary of the metalimnion. The numerical formulation
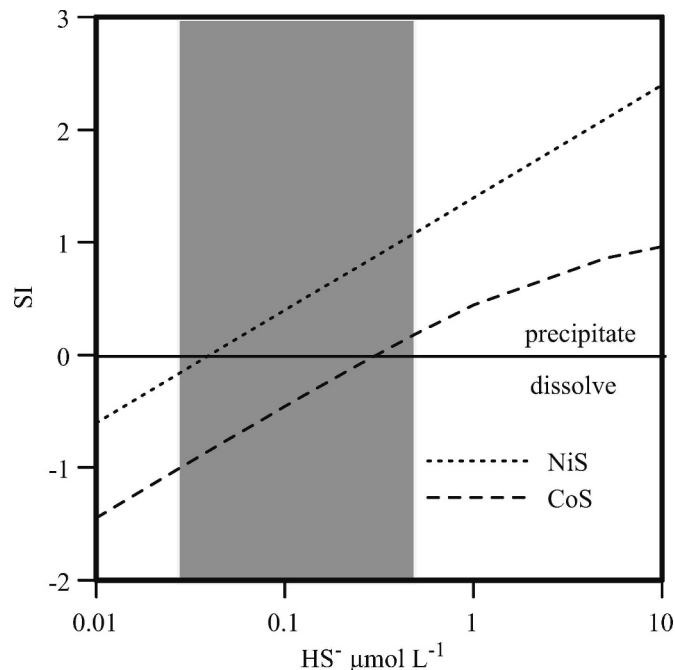
of the reaction–transport model is provided in Web Appendix 1.

The close fit between the modeled profile and the field data (Fig. 10) suggests that the Fe(II) profile is indeed shaped by an interplay between diffusion-like transport and a reaction rate that decreases approximately exponentially below the pycnocline. By fitting the measured Fe(II) profile, the value obtained for the product of the rate of Fe release to solution by reductive dissolution ($R_{Fe}(0)$) and the inverse of the coefficient of vertical eddy diffusion (K_z^{-1}) is 0.056 μmol m^{-2} (*see Web Appendix 1*).

Attempts to derive the individual values of $R_{Fe}(0)$ and K_z, however, highlight incongruencies between the field data and the one-dimensional model. For the concentrations of organic matter and particulate iron in Lake Matano, and for typical first- or second-order iron reduction kinetics (Taillefert and Gaillard 2002; Katsev et al. 2004), model-estimated values of K_z in the hypolimnion could be no less than 200 m^2 d^{-1}. Such values of K_z are unrealistic for the hypolimnion of a lake displaying a salinity gradient and a deep thermocline (Imboden and Schwarzenbach 1985).

In addition to requiring unrealistically high vertical eddy diffusivities, the one-dimensional model for dissolved Fe(II) requires that the large amount of dissolved iron diffusing upward be balanced by a high downward flux of particulate Fe(III) (Fig. 10), which is not supported by the data. The concentration of particulate (i.e., mostly ferric) iron in the vicinity of the pycnocline is several orders of magnitude smaller than the concentration of dissolved (i.e.,
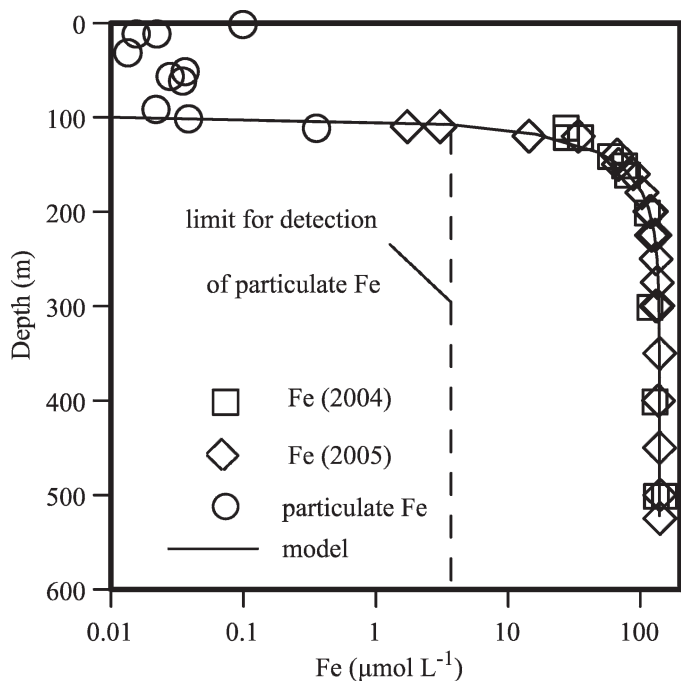
Fig. 10. The Fe(II) concentration profile generated by a one-dimensional reaction-transport model plotted with dissolved Fe(II) concentrations (2004 and 2005) and particulate Fe concentrations (2005). Note that particulate Fe concentrations could be up to 5% of the dissolved Fe concentrations below 100 m. The high limit for detection in the hypolimnetic waters is due to the limit in precision at high concentrations of dissolved Fe.

mostly ferrous) iron. If both phases are transported at comparable rates (e.g., by the same process of eddy diffusion), the quantity of particulate iron observed is insufficient to sustain the high concentrations of dissolved Fe(II) in the hypolimnion. The excess downward flux of Fe(III) required to sustain the high dissolved Fe(II) concentrations in the hypolimnion could conceivably be supplied by fast particle settling, but the particle sizes required to produce high settling rates are unrealistic (*see the following section on fluxes*). A possible explanation for the discrepancies between the model and observations is that the one-dimensional model does not take into account the potential for the sediment to act as a source or sink for dissolved and particulate Fe.

The contribution of the sediment to the exchange of Fe, Mn, P, and Cr between the epilimnion and hypolimnion can be estimated from the disparity between particulate and diffusive fluxes. In other words, discrepancies in the water column must be balanced by exchange with the sediment.

To estimate fluxes in the water column requires knowledge of the intensity of vertical eddy diffusivity (K_z). In the absence of temporal variations in temperature gradients, K_z cannot be estimated using the standard temperature method (Jassby and Powell 1975). Alternatively, we use an empirical relationship between K_z and the Brunt–Väisälä or stability frequency (N^2) (Jassby and Powell 1975). The intensity of vertical eddy diffusivity in a lake (K_z) results from the balance between the water column resistance to mixing (e.g., due to stratification) and the applied forcing (wind, density flows, seiches, etc.). The stability frequency characterizes the first part of this balance. We calculated the stability frequency for Lake Matano from the vertical density variation. Despite the variety of driving forces, in environments ranging from shallow lakes to the deep ocean, the relationship between K_z and N^2 can typically be formulated as (Lerman 1979)

$$K_z = a(N^2)^b \tag{2}$$

in which the exponent, *b,* is related to the origin and nature of turbulence and *a* is a proportionality coefficient (Jassby and Powell 1975). In the absence of data from lakes of similar size, shape, and latitude to Lake Matano, to constrain the values of *a* and *b,* we use a more general correlation (Lerman 1979). For values of $a = 3.5 \times 10^{-6}$ and $b = -1$, the relationship between K_z and N^2 appears to describe (within a factor of 5) a diverse suite of water bodies. Applying these values for the coefficients *a* and *b* and the calculated value of the stability frequency to Lake Matano reveals that the transport of solutes between epilimnion and hypolimnion at 100-m depth is character-ized by a $K_z = 0.39$ m^2 d^{-1}. This value is well within the range (0.1–10 m^2 d^{-1}) of values reported for the hypolim-nions of other lakes (Imboden and Schwarzenbach 1985).

Fluxes and the role of the sediment—Vertical fluxes of dissolved Fe, Mn, P, and Cr toward the pycnocline were calculated using measured concentration gradients and a K_z of 0.39 m^2 d^{-1} (Table 2). Fluxes of particulate species settling through the pycnocline were estimated from Stokes law (Stokes 1851) using particulate concentrations obtained from the difference between the concentrations of un-filtered and filtered samples (0.02 μm), a particle density of 2.82 g cm^{-3} (Taillefert and Gaillard 2002), and a particle size of 1 μm (De Vitre et al. 1994). These are upper estimates for particulate fluxes, since most of the particles are likely smaller than 1 μm and therefore would sink more slowly (De Vitre et al. 1994). If the one-dimensional model described in the previous section (and its analogues for

Table 2. Flux calculations.

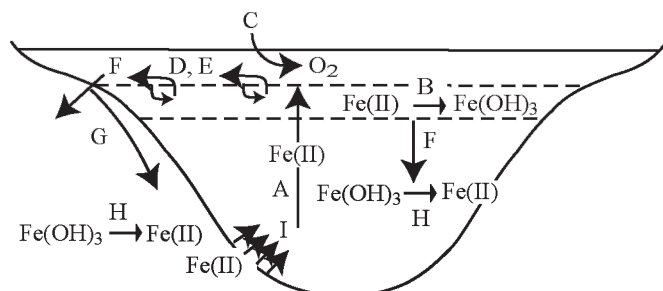| Element	Diffusive flux (μmol m^{-2} d^{-1})	Direction of diffusive flux	Particulate (μmol m^{-3})	Stokes flux (μmol m^{-2} d^{-1})	Deficit (%)
Fe	460	up	350	35	92
Mn	360	up	34	3.4	99
P	28	up	22	2.2	92
Cr	6.0	down	1	0.1	98

Fig. 11. A conceptual model for Fe cycling in Lake Matano. (A) upward diffusion of dissolved Fe(II); (B) oxidation of Fe(II) to Fe(III) followed by hydrolysis and precipitation as $Fe(OH)_3$ particles in the metalimnion; (C) diffusion of atmospheric O_2 into the epilimnion; (D, E) partial redox recycling of Fe (II) and $Fe(OH)_3$ within the metalimnion and across the pycnocline with a net lateral transport of $Fe(OH)_3$ in the epilimnion; (F) sedimentation of $Fe(OH)_3$; (G) sediment resuspension and focusing toward deeper parts of the lake; (H) reductive dissolution of $Fe(OH)_3$

dissolved Mn and P associated with Fe (hydr)oxides) were valid, the downward fluxes of particulate species should be equal to or greater than the upward fluxes of dissolved species. This is not the case, for the estimates of downward particulate fluxes of Fe, Mn, and P are more than one order of magnitude smaller than the corresponding upward diffusive fluxes (Table 2). One possible interpretation for this relies on a combination of turbulent vertical mixing in the epilimnion and horizontal mixing along isopycnals that would disperse particulate metals precipitated in the epilimnion toward the lake margins. Consequently, part of the downward return flux of particulate metals would take place in water shallower than 100 m and be captured by sediment overlain by oxygenated water. To make up for the deficit in the particulate flux, quantities of dissolved Fe, Mn, and P, equivalent to those captured by the oxic sediment, must be released from the sediments below the oxycline (i.e., below 100 m). Transport of surface sediment from oxic to anoxic depths, for example by resuspension and sediment focusing, is required to close the cycle. The overall scenario is depicted schematically in Fig. 11. Such a scenario is consistent with the steep bathymetry of the lake, which would favor downslope sediment transport (Fig. 12) and is also in line with previous observations of density currents at the lake margins (Haffner et al. 2001). The latter would resuspend particles and enhance sediment focusing. Fluctuations in the position of the redox boundary with respect to an isopleth along the lake bottom can also redistribute Fe and drive fluxes of Fe(II) into the hypolimnion (Shaffer 1986; Katsev et al. 2006). Short-term (several hours) fluctuations could result from seiching, whereas longer term fluctuations could be sustained by changes in the lake level. Such vertical excursions of the redox boundary could result in an accumulation of particulate Fe, Mn, and P in sediments above the oxycline and create an Fe-, Mn-, and P-enriched "bathtub ring." Physical modeling, based on the size and bathymetry of the lake, agrees with preliminary observations that the
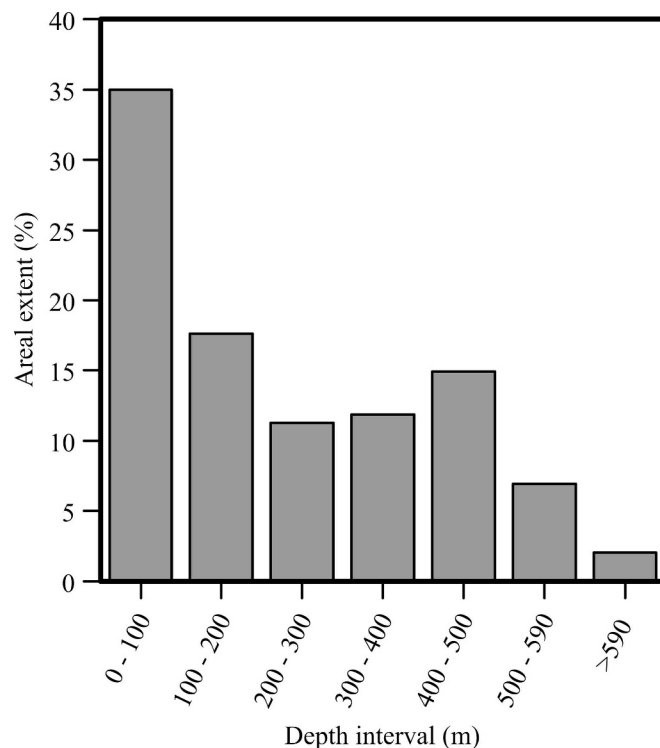

Fig. 12. Plot of the percentage areal extent of bottom sediments at different depth intervals. Sixty-five percent is below 100-m depth and is suboxic or anoxic at the sediment–water interface.

amplitude of seiches in Lake Matano may be as large as 9 m with a periodicity of several hours.

A similar reasoning can be applied to the dynamics of Cr recycling across the pycnocline. In a one-dimensional model, the downward flux of soluble Cr(VI) in the epilimnion, above the pycnocline, should be balanced by the downward flux of particulate Cr below the pycnocline. However, the particulate Cr flux is more than one order of magnitude less than the estimated downward diffusive flux above the pycnocline, which suggests that a large fraction of the Cr reduced and precipitated at the pycnocline must sediment at depths of 100 m or less.

Time scales of exchange between the epilimnion and hypolimnion—On a lake-wide scale, the value of K_z at the pycnocline can be used to estimate the time scale on which water exchanges between the epilimnion and the hypolimnion (Imboden and Schwarzenbach 1985):

$$k = \frac{K_z}{L_z^{max} h_{mix}} \quad (3)$$

where k is the rate of exchange between the epi- and hypolimnion, L_z^{max} is the maximum lake depth (590 m), and h_{mix} is the depth of the epilimnion (100 m). Based on this relationship, the time scale of exchange between the epi- and hypolimnion ($1/k$) is on the order of 400 yr if there is no large-scale convective overturn. This time scale is similar to those of temperate meromictic lakes (Imboden and Schwarzenbach 1985).

Ecological implications—According to the directions of concentration gradients at the pycnocline, exchange of water across the pycnocline should add P (and N) to the epilimnion while removing Cr(VI). Even though the gradients are steep, the exchange rate is slow. The result is low fluxes that do not favor primary production within the epilimnion. Conversely, the slow exchange allows steep concentration gradients of redox-sensitive species to develop and persist within the metalimnion. These steep gradients are conducive to the proliferation of chemoautotrophic and anoxygenic phototrophic microbial communities. Hence, in tropical lakes where the abundance of metal (hydr)oxides maintain low P concentrations in oxic waters, and where minimal seasonality precludes convective overturn and allows stable redox boundaries to develop, chemoautotrophic carbon fixation may play a comparatively larger role in the total primary production.

The large particulate Fe flux to Lake Matano may help buffer anthropogenic stresses. Sorption of phosphate on Fe (hydr)oxides precludes the accumulation of P in surface waters and eutrophication that commonly accompanies regional development (Boström et al. 1982). The potency of Fe (hydr)oxides as scavengers of divalent metals would also mitigate fluxes of Ni, Co, and other metals from the catchment soils and industrial effluents.

References

ALLISON, J. D., D. S. BROWN, AND K. J. NOVO-GRADAC. 1991. MINTEQA2/PRODEF2, A geochemical assessment model for environmental systems: Version 3.0 user's manual, p. 3–91. EPA.

ANSCHUTZ, P., S. ZHONG, B. SUNDBY, A. MUCCI, AND C. GOBEIL. 1998. Burial efficiency of phosphorus and the geochemistry of iron in continental margin sediments. Limnol. Oceanogr. **43:** 53–64.

BOSTRÖM, B., M. JANSSON, AND C. FORSBERG. 1982. Phosphorus release from lake sediments. Arch. Hydrobiol. Beih. Ergeb. Limnol. **18:** 5–59.

BRENDEL, P. J., AND G. W. LUTHER. 1995. Development of a gold amalgam voltammetric microelectrode for the determination of dissolved Fe, Mn, O-2, and S(-II) in porewaters of marine and fresh-water sediments. Environ. Sci. Technol. **29:** 751–761.

BROOKS, J. L. 1950. Speciation in ancient lakes (concluded). Quart. Rev. Biol. **25:** 131–176.

BUFFLE, J., AND W. STUMM. 1994. General chemistry of aquatic systems, p. 1–42. *In* J. Buffle and R. R. De Vitre [eds.], Chemical and biological regulation of aquatic systems. CRC.

CROWE, S. A., AND OTHERS. 2004. Biogeochemical cycling in Fe-rich sediments from Lake Matano, Indonesia, p. 1185–1189. 11th International symposium on water-rock interaction. A.A. Balkema.

DE VITRE, R. R., B. SULZBERGER, AND J. BUFFLE. 1994. Transformations of iron at redox boundaries, p. 91–137. *In* J. Buffle and R. R. Devitre [eds.], Chemical and biological regulation of aquatic systems. CRC.

GOLIGHTLY, J. P. 1981. Nickeliferous laterite deposits. Econ. Geol. **75:** 710–735.

HAFFNER, G. D., P. E. HEHANUSSA, AND D. HARTOTO. 2001. The biology and physical processes of large lakes of Indonesia, p. 183–194. *In* M. Munawar and R. E. Hecky [eds.], The great lakes of the world: Food web, health and integrity. Backhuys.

HAMILTON-TAYLOR, J., AND W. DAVISON. 1995. Redox-driven cycling of trace elements in lakes, p. 217–258. *In* A. Lerman, D. Imboden and J. Gat [eds.], Physics and chemistry of lakes. Springer.

HANSEL, C. M., B. W. WIELINGA, AND S. R. FENDORF. 2003. Structural and compositional evolution of Cr/Fe solids after indirect chromate reduction by dissimilatory iron-reducing bacteria. Geochim. Cosmochim. Acta **67:** 401–412.

HERDER, F., J. NOLTE, J. PFAENDER, J. SCHWARZER, R. K. HADIATY, AND U. K. SCHLIEWEN. 2006. Adaptive radiation and hybridization in Wallace's Dreamponds: Evidence from sailfin silversides in the Malili Lakes of Sulawesi. Proc. R. Soc. B **273:** 2209–2217.

HOPE, G. 2001. Environmental change in the Late Pleistocene and later Holocene at Wanda site, Soroako, South Sulawesi, Indonesia. Palaeogeogr. Palaeoclim. Palaeoecol. **171:** 129–145.

HUTCHINSON, G. E. 1957. A treatise on limnology: Geography, physics and chemistry. Wiley.

IMBODEN, D., AND R. P. SCHWARZENBACH. 1985. Spatial and temporal distribution of chemical substances in lakes: Modeling concepts, p. 1–28. *In* W. Stumm [ed.], Chemical processes in lakes. Wiley.

———, AND A. WÜEST. 1995. Mixing mechanisms in lakes, p. 83–138. *In* A. Lerman, D. Imboden and J. Gat [eds.], Physics and chemistry of lakes. Springer.

JASSBY, A., AND T. POWELL. 1975. Vertical patterns of eddy diffusion during stratification in Castle Lake, California. Limnol. Oceanogr. **20:** 530–543.

JOHNSON, C. A., L. SIGG, AND U. LINDAUER. 1992. The chromium cycle in a seasonally anoxic lake. Limnol. Oceanogr. **37:** 315–321.

KATSEV, S., D. G. RANCOURT, AND I. L'HEUREUX. 2004. dSED: A database tool for modeling sediment early diagenesis. Comput. Geosci. **30:** 959–967.

———, B. SUNDBY, AND A. MUCCI. 2006. Modeling vertical excursions of the redox boundary in sediments: Application to deep basins of the Arctic Ocean. Limnol. Oceanogr. **51:** 1581–1593.

KONOVALOV, S. K., AND OTHERS. 2003. Lateral injection of oxygen with the Bosporus plume—fingers of oxidizing potential in the Black Sea. Limnol. Oceanogr. **48:** 2369–2376.

LANGMUIR, D. 1997. Aqueous environmental geochemistry. Prentice-Hall Inc.

LEHMUSLUOTO, P., AND OTHERS. 1999. Limnology in Indonesia, p. 119–234. *In* R. G. Wetzel and B. Gopal [eds.], Limnology in developing countries, volume 2. International Scientific Publications.

LERMAN, A. 1979. Geochemical processes water and sediment environments. Wiley.

LEWIS, W. M. 1987. Tropical limnology. Annu. Rev. Ecol. Syst. **18:** 159–184.

LUTHER, G. W., P. J. BRENDEL, B. L. LEWIS, B. SUNDBY, L. LEFRANÇOIS, N. SILVERBERG, AND D. B. NUZZIO. 1998. Simultaneous measurement of O_2, Mn, Fe, I^-, and S(-II) in marine pore waters with a solid-state voltammetric microelectrode. Limnol. Oceanogr. **43:** 325–333.

———, B. GLAZER, S. MA, R. TROUWBORST, B. R. SHULTZ, G. DRUSCHEL, AND C. KRAIYA. 2003. Iron and sulfur chemistry in a stratified lake: Evidence for iron-rich sulfide complexes. Aquat. Geochem. **9:** 87–110.

MANCEAU, A., A. I. GORSHKOV, AND V. A. DRITS. 1992. Structural chemistry of Mn, Fe, Co, and Ni in manganese hydrous oxides. 2. Information from EXAFS spectroscopy and electron and X-Ray-diffraction. Am. Mineral. **77:** 1144–1157.

————, M. SCHLEGEL, S. RIHS, AND M. A. MARCUS. 2005. Natural speciation of Mn, Ni and Zn at the micrometer scale in a clayey paddy soil using X-ray fluorescence, absorption, and diffraction. Geochim. Cosmochim. Acta **69:** A612–A612.

————, N. TAMURA, R. S. CELESTRE, A. A. MACDOWELL, N. GEOFFROY, G. SPOSITO, AND H. A. PADMORE. 2003. Molecular-scale speciation of Zn and Ni in soil ferromanganese nodules from loess soils of the Mississippi Basin. Environ. Sci. Technol. **37:** 75–80.

MYERS, N., R. A. MITTERMEIER, C. G. MITTERMEIER, G. A. B. DA FONSECA, AND J. KENT. 2000. Biodiversity hotspots for conservation priorities. Nature **403:** 853–858.

REDFIELD, A. C., B. H. KETCHUM, AND F. A. RICHARDS. 1963. The influence of organisms on the composition of sea water, p. 26–77. *In* M. N. Hill [ed.], The sea. vol. 2. The Composition of Seawater. Wiley, New York.

REYNOLDS, C. S., S. N. REYNOLDS, I. F. MUNAWAR, AND M. MUNAWAR. 2000. The regulation of phytoplankton population dynamics in the world's largest lakes. Aquat. Ecosyst. Health Manage. **3:** 1–21.

ROY, D., M. F. DOCKER, P. HEHANUSSA, D. D. HEATH, AND G. D. HAFFNER. 2004. Genetic and morphological data supporting the hypothesis of adaptive radiation in the endemic fish of Lake Matano. J. Evol. Biol. **17:** 1268–1276.

SABO, E. M. 2006. Characterization of the pelagic plankton assemblage of Lake Matano and determination of factors regulating primary and secondary production dynamics. M.Sc. thesis, Univ. of Windsor.

SARAZIN, G., G. MICHARD, AND F. PREVOT. 1999. A rapid and accurate spectroscopic method for alkalinity measurements in sea water samples. Water Res. **33:** 290–294.

SHAFFER, G. 1986. Phosphate pumps and shuttles in the Black Sea. Nature **321:** 515–517.

SHOLKOVITZ, E. R. 1985. Redox-related geochemistry in lakes: Alkali metals, alkaline-earth elements, and ^{137}Cs, p. 119–138. *In* W. Stumm [ed.], Chemical processes in lakes. Wiley.

STOKES, G. C. 1851. On the effect of internal friction of fluids on the motion of pendulums. Trans. Cambridge Philos. Soc. **9:** 8–106.

STUMM, W., AND J. J. MORGAN. 1996. Aquatic chemistry: Chemical equilibria and rates in natural waters, 3rd ed. Wiley.

TAILLEFERT, M., AND J. F. GAILLARD. 2002. Reactive transport modeling of trace elements in the water column of a stratified lake: Iron cycling and metal scavenging. J. Hydrol. **256:** 16–34.

————, T. F. ROZAN, B. T. GLAZER, J. HERSZAGE, R. E. TROUWBORST, AND G. W. LUTHER. 2000. Seasonal variations of soluble Fe(III) in sediment porewaters as revealed by voltammetric microelectrodes. Abstr. Pap. Am. Chem. Soc. **220:** U320–U321.

U.S. ENVIRONMENTAL PROTECTION AGENCY (USEPA). 1983. Handbook for sampling and sample preservation of water and wastewater, Report No. EPA 600482029. USEPA.

U.S. ENVIRONMENTAL PROTECTION AGENCY (USEPA). 2006. National recommended water quality criteria (4304T), 25 p.U.S. Environmental Protection Agency, Office of Science and Technology.

VAN DER LEE, J. 1993. CHESS, another speciation and surface complexation computer code. CIG-Ecole des Mines de Paris.

VIOLLIER, E., P. W. INGLETT, K. HUNTER, A. N. ROYCHOUDHURY, AND P. VAN CAPPELLEN. 2000. The ferrozine method revisited: Fe(II)/Fe(III) determination in natural waters. Appl. Geochem. **15:** 785–790.

VON RINTELEN, T., AND M. GLAUBRECHT. 2003. New discoveries in old lakes: Three new species of *Tylomelania* Sarasin & Sarasin, 1897 (Gastropoda: Cerithioidea: Pachychilidae) from the Malili lake system on Sulawesi, Indonesia. J. Moll. Stud. **69:** 3–17.

WETZEL, R. G. 1983. Limnology, 2nd ed. CBS College Publishing.